Inorg. Chem. **2004**, *43*, 6609–6619

Impact of Variations in Design of Flexible Bitopic Bis(pyrazolyl)methane Ligands and Counterions on the Structures of Silver(I) Complexes: Dominance of Cyclic Dimeric Architecture

Daniel L. Reger,* Russell P. Watson, James R. Gardinier, and Mark D. Smith

Department of Chemistry and Biochemistry, University of South Carolina, Columbia, South Carolina 29208

Received July 1, 2004

The new ligands 1,1,4,4-tetra(1-pyrazolyl)butane [$CH(pz)_2(CH_2)_2CH(pz)_2$, **L2**] and 1,1,5,5-tetra(1-pyrazolyl)pentane [$CH(pz)_2(CH_2)_3CH(pz)_2$, **L3**] have been prepared to determine the structural changes in silver(I) complexes, if any, that accompany the lengthening of the spacer group between two linked bis(pyrazolyl)methane units. Silver(I) complexes of both ligands with BF_4^- and $SO_3CF_3^-$ as the counterion have the formula $[Ag_2(\mu\text{-L})_2](\text{counterion})_2$. These complexes have a cyclic dimeric structure in the solid state previously observed with the shorter linked ligand $CH(pz)_2CH_2CH(pz)_2$. Similar chemistry starting with $AgNO_3$ for **L2** yields a complex of the empirical formula $\{Ag_2[\mu\text{-}CH(pz)_2(CH_2)_2CH(pz)_2]_3\}(NO_3)_2$ that retains the cyclic dimeric structure, but bonding of an additional ligand creates a coordination polymer of the cyclic dimers. In contrast, coordination of the nitrate counterion to silver in the complex of **L3** leads to the formation of the coordination polymer of the empirical formula $[Ag(\mu\text{-}CH(pz)_2(CH_2)_3\text{-}CH(pz)_2)]NO_3$. All six new complexes have extended supramolecular structures based on noncovalent interactions supported by the counterions and the functional groups designed into the ligands.

Introduction

There is considerable interest in understanding the major factors that influence the way in which metal complexes self-assemble into supramolecular architectures.[1] The preferred coordination environment of the metal, the geometry of ligating atoms within a polynucleating ligand, and the flexibility of the ligand backbone all play key roles in directing the extended solid state structure of the resulting complex. The ability of additional functional groups built into the ligands to enter into noncovalent interactions (such as hydrogen bonding, CH···π, π···π, and cation···π) significantly impacts on the supramolecular structures of metal complexes.[2] While there are numerous systems with elegant architectures that have been produced by using noncovalent-assisted self-assembly, the general predictability of the final supramolecular structure of any given system is typically poor, especially when one considers the potential for supramolecular isomerism. Supramolecular isomerization in covalently linked coordination networks is a widely known phenomenon and has been the subject of a recent review.[3] With rigid or fixed-geometry ligands with selectively positioned donor atoms, polygons of different size or shape have been obtained, and in some cases, these polygons have been found in equilibria.[4] As the polynucleating ligand becomes

* To whom correspondence should be addressed. E-mail: reger@mail.chem.sc.edu.

(1) (a) Piguet, C.; Bernardinelli, G.; Hopfgartner, G. *Chem. Rev.* **1997**, *97*, 2005. (b) Blake, A. J.; Champness, N. R.; Hubberstey, P.; Li, W. S.; Withersby, M. A.; Schroder, M. *Coord. Chem. Rev.* **1999**, *183*, 117. (c) Batten, S. T.; Robson, R. *Angew. Chem., Int. Ed.* **1998**, *37*, 1461. (d) Leininger, S.; Olenyuk, B.; Stang, P. J. *Chem. Rev.* **2000**, *100*, 853. (e) Seidel, R. S.; Stang, P. J. *Acc. Chem. Res.* **2002**, *35*, 972. (f) Sweigers, G. F.; Malefetse, T. J. *Chem. Rev.* **2000**, *100*, 3483. (g) Zaworotko, M. J. *Chem. Commun.* **2001**, 1. (h) Dong, Y.-B.; Cheng, J.-Y.; Huang, R.-Q.; Smith, M. D.; Zur Loye, H.-C. *Inorg. Chem.* **2003**, *42*, 5699. (i) Albrecht, M. *Chem. Rev.* **2001**, *101*, 3457.

(2) (a) Khlobystov, A. N.; Blake, A. J.; Champness, N. R.; Lemenovskii, D. A.; Majouga, G.; Zyk, N. V.; Schroder, M. *Coord. Chem. Rev.* **2001**, *222*, 155. (b) Sénèque, O.; Giorgi, M.; Reinaud, O. *Chem. Commun.* **2001**, 984. (c) Weiss, H.-C.; Blaser, D.; Boese, R.; Doughan, B. M.; Haley, M. M. *Chem. Commun.* **1997**, 1703. (d) Madhavi, N. N. L.; Katz, A. K.; Carrell, H. L.; Nangia, A.; Desiraju, G. R. *Chem. Commun.* **1997**, 1953. (e) Jennings, W. B.; Farrell, B. M.; Malone, J. F. *Acc. Chem. Res.* **2001**, *34*, 885. (f) Calhorda, M. J. *Chem. Commun.* **2000**, 801. (g) Desiraju, G. R. *Acc. Chem. Res.* **1996**, *29*, 441. (h) Grepioni, F.; Cojazzi, G.; Draper, S. M.; Scully, N.; Braga, D. *Organometallics* **1998**, *17*, 296. (i) Weiss, H.-C.; Boese, R.; Smith, H. L.; Haley, M. M. *Chem. Commun.* **1997**, 2403. (j) Hunter, C. A.; Sanders, J. K. M. *J. Am. Chem. Soc.* **1990**, *112*, 5525. (k) Janiak, C. *J. Chem. Soc., Dalton Trans.* **2000**, 3885.

(3) Moulton, B.; Zaworotko, M. J. *Chem. Rev.* **2001**, *101*, 1629.

(4) (a) Schweiger, M.; Seidel, S. R.; Arif, A. M.; Stang, P. J. *Inorg. Chem.* **2002**, *41*, 2556. (b) Cotton, F. A.; Daniels, L. M.; Lin, C.; Murillo, C. A. *J. Am. Chem. Soc.* **1999**, *121*, 4538.

10.1021/ic0491377 CCC: $27.50
Published on Web 09/16/2004

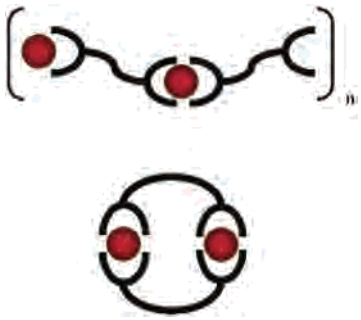

Figure 1. Potential supramolecular isomers based on flexible bidentate ligands and tetrahedral metal centers.

more flexible[5] and capable of participating in more noncovalent interactions, the resulting predictability of the supramolecular structure decreases even further. At a minimum, flexible ligands can exhibit the same type of supramolecular isomerism exhibited by their more rigid counterparts as in Figure 1. Their flexibility, however, allows the ligand backbone to maximize the number of noncovalent contacts, and the resultant extended structures often lead to strikingly pleasing but numerous architectures that can be altered by subtle changes in the system such as varying the solvent or counterion.[6] This strategy has been exploited recently where it was found to be possible to tune the apparent strength of transannular silver···silver interactions in $\{Ag_2[\mu\text{-}[(4\text{-py})SiMe_2]_2O]_2^{2+}\}$ simply by substituting anions.[7] One major goal in coordination polymer/network research (or in 'crystal engineering') is to try to achieve a greater degree of predictability in the extended structures in these latter flexible systems by rational substitution of the ligand backbones, the metal centers, and the counterions.

Our group has recently prepared a new series of multitopic ligands designed to support supramolecular structures. The ligands are based on poly(pyrazolyl)methane units which are capable of multiple binding modes and that also have the potential to participate in important noncovalent interactions that direct their self-assembly into remarkable architectures. Our initial work was linking tris(pyrazolyl)methane units with semirigid groups to prepare the ligands $C_6H_{6-n}[CH_2OCH_2C(pz)_3]_n$ (n = 2, 3, 4, 6; pz = pyrazol-1-yl), and study the structures of their metal complexes.[8] We are currently developing linked ligands based on bis(pyrazolyl)methane units linked by rigid,[9] semirigid,[10] and flexible[11] organic spacers. We are interested in how different types of linking groups as well as differing poly(pyrazolyl)methane units impact on the coordination and supramolecular structures of a variety of metal complexes. We are also studying the impact of various counterions on the supramolecular structures.[8a,e]

We previously reported the synthesis of a methylene-linked bis(pyrazolyl)methane ligand, $CH_2[CH(pz)_2]_2$ (**L1**),[11] along with its 4-ethylpyrazolyl substituted derivative, $CH_2[CH(pz^{4Et})_2]_2$ (pz^{4Et} = 4-ethylpyrazol-1-yl) (**L1^{4Et}**).[12] Preliminary studies on the coordination chemistry of these first generation linked bis(pyrazolyl)methane ligands with silver(I) salts led to some interesting observations. First, the isolated products from the equimolar reactions between these ligands and either $AgSO_3CF_3$ or $AgNO_3$ had the following formulas: $[Ag_2(\mathbf{L1})_2](SO_3CF_3)_2$, $[Ag_3(\mathbf{L1})_2](NO_3)_3$, and $[Ag_2(\mathbf{L1}^{4Et})_2]_3[Ag(NO_3)_4]_2$. The $AgSO_3CF_3$ complex of **L1** formed discrete cyclic dimers in which two **L1** ligands bridged two silver cations whereas the $AgNO_3$ complex crystallized as an unusual acyclic trimetallic zwitterionic species where two ligands bridged three silvers. The $AgNO_3$ complex of **L1^{4Et}** formed discrete cyclic dimeric cations analogous to those of the $AgSO_3CF_3$ complex of **L1**, but in this case the unusual $[Ag(NO_3)_4]^{3-}$ trianion was formed. These results are in line with the greater proclivity of $AgNO_3$ to give unpredictable coordination complexes with more unusual coordination geometries when compared to silver derivatives with noncoordinating anions.[13] Second, in these studies involving other linked bis- and tris(pyrazolyl)methane ligands, many of the complexes had highly organized supramolecular structures involving an important cooperative noncovalent interaction between the pyrazolyl rings. In this interaction, four pyrazolyl rings are associated through CH···π and π···π interactions as shown in Figure 2. A survey of the Cambridge Structural Database revealed this to be a common

(5) (a) Müller, I. M.; Röttgers, T.; Sheldrik, W. S.; *Chem. Commun.* **1998**, 823. (b) Black, J. R.; Champness, N. R.; Levason, W.; Reid, G. *Inorg. Chem.* **1996**, *35*, 4432. (c) Blake, A. J.; Li, W.-S.; Lippolis, V.; Schröder, M. *Chem Commun.* **1997**, 1943.

(6) (a) Blake, A. J.; Champness, N. R.; Cooke, P. A.; Nicolson, J. E. B. *Chem. Commun.* **2000**, 665. (b) Hirsch, K. A.; Wilson, S. R.; Moore, J. S. *Inorg. Chem.* **1997**, *36*, 2960. (c) Blake, A. J.; Champness, N. R.; Cooke, P. A.; Nicolson, J. E. B.; Wilson, C. *J. Chem. Soc., Dalton Trans.* **2000**, 3811. (d) Yang, S.-P.; Chen, X.-M.; Ji, L.-N. *J. Chem. Soc., Dalton Trans.* **2000**, 2337. (e) Fei, B.-L.; Sun, W.-Y.; Yu, K.-B.; Tang, W.-X. *J. Chem. Soc., Dalton Trans.* **2000**, 805. (f) Paul, R. L.; Couchman, S. M.; Jeffery, J. C.; McCleverty, J. A.; Reeves, Z. R.; Ward, M. D. *J. Chem. Soc., Dalton Trans.* **2000**, 865. (g) Vilar, R.; Mingos, D. M.; White, A. J. P.; Williams, D. J. *Angew. Chem., Int. Ed.* **1998**, *37*, 1258. (h) Hong, M.; Su, W.; Cao, R.; Fujita, M.; Lu, J. *Chem. Eur. J.* **2000**, *6*, 427. (i) Withersby, M. A.; Blake, A. J.; Champness, N. R.; Cooke, P. A.; Hubberstey, P.; Li, W.-S.; Schröder, M. *Inorg. Chem.* **1999**, *38*, 2259. (j) Lu, J.; Paliwala, T.; Lim, S. C.; Yu, C.; Niu, T.; Jacobson, A. J. *Inorg. Chem.* **1997**, *36*, 923. (k) Reger, D. L.; Semeniuc, R. F.; Smith, M. D. *Eur. J. Inorg. Chem.* **2003**, 3480. (l) Hannon, M. J.; Painting, C. L.; Plummer, E. A.; Childs, L. J.; Alcock, N. W. *Chem. Eur. J.* **2002**, *8*, 2225.

(7) Jung, O.-S.; Kim, Y. J.; Lee, Y. J.; Kang, S. W.; Choi, S. N. *Cryst. Growth. Des.* **2004**, *4*, 23.

(8) (a) Reger, D. L.; Semeniuc, R. F.; Rassolov, V.; Smith, M. D. *Inorg. Chem.* **2004**, *43*, 537. (b) Reger, D. L.; Semeniuc, R. F.; Smith, M. D. *Inorg. Chem.* **2003**, *42*, 8137. (c) Reger, D. L.; Semeniuc, R. F.; Silaghi-Dumitrescu, I.; Smith, M. D. *Inorg. Chem.* **2003**, *42*, 3751. (d) Reger, D. L.; Semeniuc, R. F.; Smith, M. D. *J. Chem. Soc., Dalton Trans.* **2003**, 285. (e) Reger, D. L.; Semeniuc, R. F.; Smith, M. D. *J. Organomet. Chem.* **2003**, *666*, 87. (f) Reger, D. L.; Brown, K. J.; Smith, M. D. *J. Organomet. Chem.* **2002**, *658*, 50. (g) Reger, D. L.; Semeniuc, R. F.; Smith, M. D. *Eur. J. Inorg. Chem.* **2002**, 543. (h) Reger, D. L.; Semeniuc, R. F.; Smith, M. D. *J. Chem. Soc., Dalton Trans.* **2002**, 476. (i) Reger, D. L.; Semeniuc, R. F.; Smith, M. D. *Inorg. Chem.* **2001**, *40*, 6545.

(9) Reger, D. L.; Gardinier, J. R.; Smith, M. D. *Polyhedron* **2004**, *23*, 291−299.

(10) Reger, D. L.; Brown, K. J.; Gardinier, J. R.; Smith, M. D. *Organometallics* **2003**, *22*, 4973.

(11) Reger, D. L.; Gardinier, J. R.; Semeniuc, R. F.; Smith, M. D. *J. Chem. Soc., Dalton Trans.* **2003**, 1712.

(12) Reger, D. L.; Gardinier, J. R.; Grattan, T. C.; Smith, M. R.; Smith, M. D. *New J. Chem.* **2003**, *27*, 1670.

(13) (a) McMorran, D. A.; Pfadenhauer, S.; Steel, P. J. *Aust. J. Chem.* **2002**, *23*, 519. (b) Steel, P. J.; Sumby, C. J. *Inorg. Chem. Commun.* **2002**, *5*, 323.

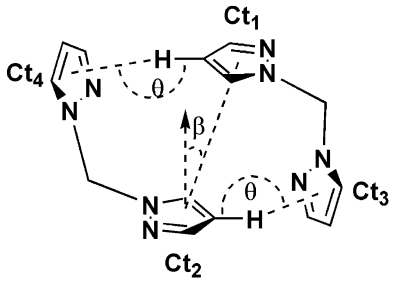

Figure 2. Geometric parameters associated with the quadruple pyrazolyl embrace: Ct = ring centroid, β = angle between the ring normal and centroid−centroid vector, θ = CH···Ct angle in the CH···π interactions.

motif for poly(pyrazolyl)methane and -borate compounds, and we have termed this interaction the "quadruple pyrazolyl embrace."[11]

We were interested in determining the structural impact not only of changing the length of the alkylidene spacer between the bis(pyrazolyl)methane ligating sites but also of changing the anions. We first wanted to establish whether longer chain derivatives of **L1** would produce silver complexes whose structures were based on discrete cyclic cationic units as observed for the complexes of **L1** and **L1^{4Et}** or instead were based on acyclic species or coordination polymers, as seen in the complexes of $Fe\{C_5H_4[CH(pz)_2]\}_2$[10] and in other systems.[1g,6k,l,8c,d,i,14] We were also interested in exploring how variation in the anions of the silver complexes would influence the solid state structure, with a particular interest in the potentially fascinating coordination chemistry involving the nitrate anion. More importantly, we were interested in trying to elucidate what factors were responsible for either promoting or inhibiting the pyrazolyl embrace as it occurs in about 25% of all cases in poly(pyrazolyl)borate and -methane chemistry. Herein, we report the syntheses of the ethylene- and propylene-linked bis(pyrazolyl)methane ligands 1,1,4,4-tetra(1-pyrazolyl)butane (**L2**) and 1,1,5,5-tetra(1-pyrazolyl)pentane (**L3**), their respective $AgBF_4$, $AgSO_3CF_3$, and $AgNO_3$ complexes, and the supramolecular structures of these complexes.

Experimental Section

General Comments. Air-sensitive materials were handled under a nitrogen atmosphere using standard Schlenk techniques or in a Vacuum Atmospheres HE-493 drybox. All solvents were dried and distilled by conventional methods prior to use. Reported melting points are uncorrected. IR spectra were obtained on a Nicolet 5DXBO FTIR spectrometer. The ^{1}H,^{13}C, and ^{19}F NMR spectra were recorded on a Varian AM300 or Varian AM400 spectrometer. All chemical shifts are in ppm and were referenced to solvent signals. Mass spectrometric measurements were obtained on a MicroMass QTOF spectrometer or on a VG 70S instrument. Elemental analyses were performed on vacuum-dried samples by Robertson Microlit Laboratories (Madison, NJ). Commercially available chemicals were purchased from Aldrich or Fisher Scientific. Pyrazole was purified by sublimation prior to use. All other purchased chemicals were used as received. Glutaraldehyde bis(dimethylacetal) was prepared by a reported procedure.[15]

Succinaldehyde Bis(dimethylacetal). Gaseous HCl (generated by dropwise addition of H_2SO_4 on NaCl) was bubbled through 30 mL of absolute methanol while cooled in an ice−water bath for 45 min. 2,5-Dimethoxytetrahydrofuran (5 g, 37.8 mmol) was then added in one portion and the solution heated at gentle reflux for 4 h, during which time the color changed from bright yellow to opaque black. After cooling to room temperature, the solution was neutralized with aqueous NaOH and extracted with CH_2Cl_2 (3 × 30 mL). The combined organic extracts were washed with saturated NH_4Cl (50 mL), dried over $MgSO_4$, and filtered. Removal of the solvent yielded a dark red-brown liquid that was distilled under dynamic vacuum (1 mmHg). The fraction collected at 47 °C was the desired bis(dimethylacetal). Yield = 4.05 g (60%). IR (liquid film, cm^{-1}): 2938, 2901, 2823, 2668, 1446, 1385, 1356, 1250, 1185, 1119, 1062, 952. ^{1}H NMR (300 MHz, $CDCl_3$): δ 4.35 (br s, 2 H, C*H*(OCH$_3$)$_2$), 3.29 (s, 12 H, OC*H*$_3$), 1.64−1.62 (m, 4 H, C*H*$_2$C*H*$_2$).^{13}C NMR (75.5 MHz, $CDCl_3$): δ 104.13, 52.68, 27.50. HRMS: Direct probe (*m*/*z*) calcd for $C_8H_{17}O_4$ $[M - H]^+$ 177.1127, found 177.1130. Direct probe MS *m*/*z* (rel int %) [assgn]: 177 (1) $[M - H]^+$, 147 (5) $[M - CH_3OH]^+$, 115 (50) $[M - 2CH_3OH]^+$, 75 (100) $[CH(OCH_3)_2]^+$.

CH(pz)$_2$(CH$_2$)$_2$CH(pz)$_2$, 1,1,4,4-Tetra(1-pyrazolyl)butane (L2). Succinaldehyde bis(dimethylacetal) (2.96 g, 16.6 mmol), pyrazole (4.52 g, 66.4 mmol), and *p*-toluenesulfonic acid monohydrate (0.253 g, 1.33 mmol) were combined in a flask equipped with a short-path distillation column attached to a tared vial to monitor the evolution of methanol. With heating, the solids dissolved in the acetal. Heating was continued until 2.2 mL of methanol had been collected (theoretical yield = 2.7 mL). The product solution solidified on cooling to room temperature. It was dissolved in 400 mL of CH_2Cl_2 and stirred for several minutes with 50 mL of 4% aqueous Na_2CO_3. The layers were separated, and the aqueous phase was extracted with CH_2Cl_2 (2 × 30 mL). The combined organic extracts were washed with concentrated aqueous NaCl and dried over $MgSO_4$. Upon removal of the solvent, an off-white solid remained that was recrystallized from absolute ethanol. Yield = 2.79 g (52%). Mp = 192−193 °C. Anal. Calcd for $C_{16}H_{18}N_8$: C, 59.61; H, 5.63; N, 34.76. Found: C, 59.58; H, 5.54; N, 34.84. IR (KBr, cm^{-1}): 3134, 3109, 3015, 2954, 2888, 1634, 1516, 1430, 1397. ^{1}H NMR (400 MHz, $CDCl_3$): δ 7.57 (d, J = 2.4 Hz, 4 H, 5-H pz), 7.53 (d, J = 1.6 Hz, 4 H, 3-H pz), 6.40 (s, 2 H, C*H*(pz)$_2$), 6.26 (dd, J = 2.4, 2.0 Hz, 4 H, 4-H pz), 2.60−2.59 (m, 4 H, C*H*$_2$C*H*$_2$). ^{1}H NMR (300 MHz, CD_3CN): δ 7.69 (dd, J = 2.3, 0.9 Hz, 4 H, 5-H pz), 7.47 (d, J = 1.8 Hz, 4 H, 3-H pz), 7.48 (br s, 2 H, C*H*(pz)$_2$), 6.25 (dd, J = 2.6, 1.8 Hz, 4 H, 4-H pz), 2.47−2.45 (m, 4 H, C*H*$_2$C*H*$_2$). ^{13}C NMR (75.5 MHz, $CDCl_3$): δ 140.3, 128.5, 106.8, 74.9, 29.9. HRMS: Direct probe (*m*/*z*) calcd for $C_{16}H_{18}N_8$ 322.1654, found 322.1651. Direct probe MS *m*/*z* (rel int %) [assgn]: 322 (1) $[M]^+$, 254 (25) $[M - Hpz]^+$, 187 (55) $[M - Hpz - pz]^+$, 119 (100) $[M - 2Hpz - pz]^+$.

CH(pz)$_2$(CH$_2$)$_3$CH(pz)$_2$, 1,1,5,5-Tetra(1-pyrazolyl)pentane (L3). Glutaraldehyde bis(dimethylacetal), pyrazole (8.19 g, 0.120 mol), and *p*-toluenesulfonic acid monohydrate (0.455 g, 2.39 mmol) were combined in a flask equipped with a short-path distillation column attached to a tared vial to monitor the evolution of methanol. Upon heating, the solids dissolved in the acetal. Heating was continued

(14) (a) Hong, M.; Zhao, Y.; Su, W.; Cao, R.; Fujita, M.; Zhou, Z.; Chan, A. S. C. *Angew. Chem., Int. Ed.* **2000**, *39*, 2468. (b) Muthu, S.; Yip, J. H. K.; Vittal, J. J. *J. Chem. Soc., Dalton Trans.* **2002**, 4561. (c) Itaya, T.; Inoue, K. *Polyhedron* **2002**, *21*, 1573. (d) Blake, A. J.; Baum, G.; Champness, N. R.; Chung, S. S. M.; Cooke, P. A.; Fenske, D.; Khlobystov, A. N.; Lemenovskii, D. A.; Li, W.-S.; Schröder, M. *J. Chem. Soc., Dalton Trans.* **2000**, 4285. (e) Battan, S. R.; Jeffery, J. C.; Ward, M. D. *Inorg. Chim. Acta* **1999**, *292*, 231.

(15) Gosselin, P.; Rouessac, F.; Zamarlik, H. *Bull. Soc. Chim. Fr.* **1981**, 192.

until 4.2 mL of methanol had been collected (theoretical yield = 4.9 mL). The product solution solidified on cooling to room temperature. It was dissolved in 30 mL of CH_2Cl_2 and stirred for several minutes with 50 mL of 4% aqueous Na_2CO_3. The layers were separated, and the aqueous phase was extracted with CH_2Cl_2 (3 × 20 mL). The combined extracts were washed with concentrated aqueous NaCl and dried over $MgSO_4$. The crude product was chromatographed (silica gel, Et_2O) and recrystallized from absolute ethanol to afford 7.28 g (72%) of a white solid. Mp: 113−114 °C. Anal. Calcd for $C_{17}H_{20}N_8$: C, 60.70; H, 5.99; N, 33.31. Found: C, 60.38; H, 6.15; N, 33.13. IR (KBr, cm^{-1}): 3130, 3109, 3011, 2983, 2966, 2942, 2868, 1761, 1724, 1605, 1511, 1442. ^{1}H NMR (400 MHz, $CDCl_3$): δ 7.58 (dd, J = 2.4, 0.4 Hz, 4 H, 5-H pz), 7.52 (dd, J = 1.8, 0.4 Hz, 4 H, 3-H pz), 6.34 (t, J = 7.6 Hz, 2 H, C*H*(pz)$_2$), 6.25 (dd, J = 2.4, 2.0 Hz, 4 H, 4-H pz), 2.66 (q, J = 7.6 Hz, 4 H, CH_2CH$_2$CH_2), 1.27−1.20 (m, 2 H, CH$_2$CH_2CH$_2$).^{1}H NMR (300 MHz, CD_3CN): δ 7.70 (d, J = 2.4 Hz, 4 H, 5-H pz), 7.43 (d, J = 1.5 Hz, 4 H, 3-H pz), 6.41 (t, J = 7.7 Hz, 2 H, C*H*(pz)$_2$), 6.22 (dd, J = 2.3, 1.7 Hz, 4 H, 4-H pz), 2.59 (q, J = 7.8 Hz, 4 H, CH_2CH$_2$CH_2), 1.16−1.05 (m, 2 H, CH$_2$CH_2CH$_2$). ^{13}C NMR (75.5 MHz, $CDCl_3$): δ 140.0, 128.3, 106.6, 75.2, 33.0, 21.0. HRMS: Direct probe (*m*/*z*) calcd for $C_{17}H_{20}N_8$ 336.1811, found 336.1806. Direct probe MS *m*/*z* (rel int %) [assgn]: 336 (1) [M]$^+$, 268 (10) [M − Hpz]$^+$, 201 (75) [M − Hpz − pz]$^+$, 133 (35) [M − 2Hpz − pz]$^+$, 107 (100) [M − 2Hpz − CH_2CHpz]$^+$.

Silver Complexes. Silver complexes of the two ligands were prepared by dissolving the silver salt and the ligand together in CH_3CN or CH_2Cl_2 and crystallizing by vapor diffusion of diethyl ether into these solutions. Single crystals used for XRD analysis were taken directly from the mother liquor. All other crystals were removed from the mother liquor, rinsed with diethyl ether, and dried before characterization. Yields are based on equimolar starting amounts of the ligand and respective silver salt (0.310 mmol for the ethylene-linked ligand; 0.297 mmol for the propylene-linked ligand).

[Ag$_2$(μ-CH(pz)$_2$(CH$_2$)$_2$CH(pz)$_2$)$_2$](BF$_4$)$_2$·0.5CH$_3$CN (1). Crystallized from CH_3CN/Et_2O. Yield = 108 mg (67%). Mp: 259−261 °C. Anal. Calcd for $C_{33}H_{37.5}Ag_2B_2F_8N_{16.5}$: C, 37.58; H, 3.58; N, 21.91. Found: C, 37.81; H, 3.60; N, 21.62. IR (KBr, cm^{-1}): 3138, 3125, 3015, 1516, 1442, 1401, 1295, 1058. ^{1}H NMR (300 MHz, CD_3CN): δ 7.82 (dd, J = 2.7, 0.6 Hz, 4 H, 5-H pz), 7.43 (d, J = 2.1 Hz, 4 H, 3-H pz), 6.61 (br s, 2 H, C*H*(pz)$_2$), 6.31 (t, J = 2.3 Hz, 4 H, 4-H pz), 2.59−2.56 (m, 4 H, CH_2CH_2).^{13}C NMR (75.5 MHz, CD_3CN): δ 143.6, 132.7, 107.8, 75.1, 30.4. ^{19}F NMR (376 MHz, CD_3CN): δ −151.58 (s, 25% rel int), −151.63 (s, 100% rel int). HRMS: ESI(+) (*m*/*z*) calcd for $C_{32}H_{36}Ag_2BF_4N_{16}$, [Ag$_2$(**L2**)$_2BF_4$]$^+$ 947.1444, found 947.1447. ESI(+) MS *m*/*z* (rel int %) [assgn]: 947 (15) [Ag$_2$(**L2**)$_2$BF$_4$]$^+$, 753 (5) [Ag(**L2**)$_2$]$^+$, 470 (30) [Ag(**L2**)(CH$_3$CN)]$^+$, 429 (100) [Ag(**L2**)]$^+$.

[Ag$_2$(μ-CH(pz)$_2$(CH$_2$)$_2$CH(pz)$_2$)$_2$](SO$_3$CF$_3$)$_2$·0.5CH$_2$Cl$_2$ (2). Crystallized from CH_2Cl_2/Et_2O. Yield = 75 mg (40%). Mp: 242−243 °C. Anal. Calcd for $C_{34}H_{36}Ag_2F_6N_{16}O_6S_2$: C, 35.25; H, 3.13; N, 19.34. Found: C, 35.12; H, 2.87; N, 19.05. IR (KBr, cm^{-1}): 3142, 3125, 3105, 2995, 1516, 1450, 1401, 1270, 1164. ^{1}H NMR (300 MHz, CD_3CN): δ 7.79 (d, J = 2.1 Hz, 4 H, 5-H pz), 7.45 (d, J = 1.8 Hz, 4 H, 3-H pz), 6.59 (br s, 2 H, C*H*(pz)$_2$), 6.30 (t, J = 2.3 Hz, 4 H, 4-H pz), 2.56−2.53 (m, 4 H, CH_2CH_2).^{13}C NMR (75.5 MHz, CD_3CN): δ 143.7, 132.8, 107.8, 75.1, 30.4.^{19}F NMR (376 MHz, CD_3CN): δ −79.65 (s). HRMS: ESI(+) (*m*/*z*) calcd for $C_{33}H_{36}Ag_2F_3N_{16}O_3S$, [Ag$_2$(**L2**)$_2SO_3CF_3$]$^+$ 1009.0930, found 1009.0938. ESI(+) MS *m*/*z* (rel int %) [assgn]: 1009 (20) [Ag$_2$(**L2**)$_2$SO$_3$CF$_3$]$^+$, 751 (5) [Ag(**L2**)$_2$]$^+$, 470 (30) [Ag(**L2**)(CH$_3$CN)]$^+$, 429 (100) [Ag(**L2**)]$^+$.

[Ag$_2$(μ-CH(pz)$_2$(CH$_2$)$_2$CH(pz)$_2$)$_3$](NO$_3$)$_2$ (3). Crystallized from CH_3CN/Et_2O. Yield = 64 mg (47%). Mp: 229−230 °C. Anal. Calcd for $C_{48}H_{54}Ag_2N_{26}O_6$: C, 44.12; H, 4.16; N, 27.87. Found: C, 43.84; H, 3.84; N, 27.64. IR (KBr, cm^{-1}): 3101, 2991, 1753, 1512, 1458, 1381, 1320, 1156, 1091, 1046, 874, 768, 617. ^{1}H NMR (300 MHz, CD_3CN): δ 7.72 (d, J = 2.1 Hz, 4 H, 5-H pz), 7.49 (d, J = 2.1 Hz, 4 H, 3-H pz), 6.51 (br s, 2 H, C*H*(pz)$_2$), 6.27 (dd, J = 2.4, 2.1 Hz, 4 H, 4-H pz), 2.48−2.46 (m, 4 H, CH_2CH_2). ESI(+) MS *m*/*z* (rel int %) [assgn]: 922 (10) [Ag$_2$(**L2**)$_2$NO$_3$]$^+$, 751 (10) [Ag(**L2**)$_2$]$^+$, 470 (25) [Ag$_2$(**L2**)$_2$CH$_3$CN]$^{2+}$, 429 (100) [Ag(**L2**)]$^+$.

[Ag$_2$(μ-CH(pz)$_2$(CH$_2$)$_3$CH(pz)$_2$)$_2$](BF$_4$)$_2$ (4). Crystallized from CH_3CN/Et_2O. Yield = 103 mg (65%). Mp: 249−251 °C. Anal. Calcd for $C_{34}H_{40}Ag_2B_2F_8N_{16}$: C, 38.45; H, 3.80; N, 21.10. Found: C, 38.32; H, 3.49; N, 21.17. IR (KBr, cm^{-1}): 3141, 3125, 3019, 2954, 2929, 1520, 1450, 1401, 1295, 1074, 756. ^{1}H NMR (300 MHz, CD_3CN): δ 7.77 (d, J = 2.7 Hz, 4 H, 5-H pz), 7.53 (d, J = 1.8 Hz, 4 H, 3-H pz), 6.49 (t, J = 7.8 Hz, 2 H, C*H*(pz)$_2$), 6.30 (t, J = 2.1 Hz, 4 H, 4-H pz), 2.61 (q, J = 7.8, 4 H, CH_2CH$_2$CH_2), 1.04−1.01 (m, 2 H, CH$_2$CH_2CH$_2$).^{13}C NMR (75.5 MHz, CD_3CN): δ 143.0, 131.9, 107.7, 75.4, 33.6, 21.7. ^{19}F NMR (376 MHz, CD_3CN): δ −151.95 (s, 25% rel int), −152.01 (s, 100% rel int). HRMS: ESI(+) (*m*/*z*) calcd for $C_{34}H_{40}Ag_2BF_4N_{16}$, [Ag$_2$(**L3**)$_2BF_4$]$^+$ 975.1758, found 975.1758. ESI(+) MS *m*/*z* (rel int %) [assgn]: 975 (1) [Ag$_2$(**L3**)$_2$BF$_4$]$^+$, 779 (1) [Ag(**L3**)$_2$]$^+$, 443 (100) [Ag(**L3**)]$^+$.

[Ag$_2$(μ-CH(pz)$_2$(CH$_2$)$_3$CH(pz)$_2$)$_2$](SO$_3$CF$_3$)$_2$·2CH$_2$Cl$_2$ (5). Crystallized from CH_2Cl_2/Et_2O. Yield = 74 mg (37%). Mp: 173−174 °C. Anal. Calcd for $C_{36}H_{40}Ag_2F_6N_{16}O_6S_2$: C, 36.44; H, 3.40; N, 18.89. Found: C, 36.46; H, 3.11, N, 19.08. IR (KBr, cm^{-1}): 3117, 2991, 2958, 2958, 1512, 1446, 1397, 1262, 1164, 1025.^{1}H NMR (300 MHz, CD_3CN): δ 7.76 (d, J = 2.7 Hz, 4 H, 5-H pz), 7.52 (d, J = 1.5 Hz, 4 H, 3-H pz), 6.48 (t, J = 7.5 Hz, 2 H, C*H*(pz)$_2$), 6.28 (t, J = 2.3 Hz, 4 H, 4-H pz), 2.61 (q, J = 7.8, 4 H, CH_2CH$_2$CH_2), 1.05−1.01 (m, 2 H, CH$_2$CH_2CH$_2$). ^{13}C NMR (75.5 MHz, CD_3CN): δ 142.6, 131.6, 107.6, 75.5, 33.6, 21.7.^{19}F NMR (376 MHz, CD_3CN): δ −79.73 (s). HRMS: ESI(+) (*m*/*z*) calcd for $C_{35}H_{40}Ag_2F_3N_{16}O_3S$, [Ag$_2$(**L3**)$_2SO_3CF_3$]$^+$ 1037.1251, found 1037.1243. ESI(+) MS *m*/*z* (rel int %) [assgn]: 1037 (2) [Ag$_2$(**L3**)$_2$SO$_3$CF$_3$]$^+$, 443 (100) [Ag(**L3**)]$^+$.

[Ag(CH(pz)$_2$(CH$_2$)$_3$CH(pz)$_2$)]NO$_3$ (6). Crystallized from CH_3CN/Et_2O. Yield = 128 mg (83%). Mp: 205−207 °C. Anal. Calcd for $C_{17}H_{20}AgN_9O_3$: C, 40.33; H, 3.98; N, 24.90. Found: C, 40.19; H, 3.62; N, 24.17. IR (KBr, cm^{-1}): 3117, 2942, 2921, 2860, 1736, 1610, 1520, 1442, 1401, 1291, 1103, 1042, 972, 919, 890, 760, 617 cm^{-1}. ^{1}H NMR (300 MHz, CD_3CN): δ 7.79 (dd, J = 2.4, 0.9 Hz, 4 H, 5-H pz), 7.51 (d, J = 1.8 Hz, 4 H, 3-H pz), 6.53 (t, J = 7.7 Hz, 2 H, C*H*(pz)$_2$), 6.28 (t, J = 2.0 Hz, 4 H, 4-H pz), 2.62 (q, J = 7.8, 4 H, CH_2CH$_2$CH_2), 1.05−0.99 (m, 2 H, CH$_2$CH_2CH$_2$).^{13}C NMR (75.5 MHz, DMSO-d_6): δ 140.5, 130.0, 106.1, 73.5, 32.0, 20.3. HRMS: ESI(+) (*m*/*z*) calcd for $C_{17}H_{20}AgN_8$, [Ag(**L3**)]$^+$ 443.0862, found 443.0875. ESI(+) MS *m*/*z* (rel int %) [assgn]: 443 (100) [Ag(**L3**)]$^+$, 337 (10) [**L3**]$^+$.

Crystal Structure Determinations. X-ray intensity data from a colorless bar of **1**, an irregular colorless fragment cleaved from a larger crystal of **2**, a colorless block of **3**, a colorless plate of **4**, and colorless prisms of **5** and **6** were measured at 150(1) K for all but **3** which was at 294(1) K on a Bruker SMART APEX CCD-based diffractometer (Mo Kα radiation, λ = 0.71073 Å).[16] All crystals were taken directly from the crystallizing containers. Raw data frame integration and Lp corrections were performed with SAINT+.[16] Final unit cell parameters were determined by least-

(16) *SMART* version 5.625, *SAINT+* version 6.22, and *SADABS* version 2.05; Bruker Analytical X-ray Systems, Inc.: Madison, WI, 2001.

Table 1. Crystal Data and Refinement Details for Compounds **1**−**6**

	1	**2**	**3**	**4**	**5**	**6**
empirical formula	$C_{33}H_{37.5}Ag_2B_2F_8N_{16.5}$	$C_{34.5}H_{37}Ag_2ClF_6N_{16}O_6S_2$	$C_{48}H_{54}Ag_2N_{26}O_6$	$C_{17}H_{20}AgBF_4N_8$	$C_{38}H_{44}Ag_2Cl_4F_6N_{16}O_6S_2$	$C_{17}H_{20}AgN_9O_3$
fw	1054.66	1201.11	1306.91	531.09	1356.55	506.29
T (K)	150(2)	150(2)	294(2)	150(1)	150(1)	150(2)
cryst syst	triclinic	monoclinic	monoclinic	triclinic	monoclinic	monoclinic
space group	$P\bar{1}$	$C2/c$	$P2_1/c$	$P\bar{1}$	$P2_1/n$	$P2_1/c$
a, Å	9.4745(6)	40.782(2)	8.3629(4)	13.0016(8)	12.6354(6)	8.9678(5)
b, Å	11.2647(7)	11.1242(6)	17.6037(8)	14.3671(9)	15.4554(8)	13.0984(8)
c, Å	21.5642(13)	21.7275(11)	19.1867(8)	14.4522(9)	14.7501(7)	16.7159(10)
α, deg	88.4010(10)	90	90	71.6430(10)	90	90
β, deg	84.2380(10)	102.2470(10)	101.0000(10)	65.4890(10)	112.4360(10)	90.0980(10)
γ, deg	65.8370(10)	90	90	63.9800(10)	90	90
V, Å^3	2089.0(2)	9632.7(9)	2772.7(2)	2178.0(2)	2662.4(2)	1963.5(2)
Z	2	8	2	4	2	4
D (calcd) Mg·m^{-3}	1.677	1.656	1.565	1.620	1.692	1.713
abs coeff, mm^{-1}	1.022	1.038	0.780	0.980	1.095	1.068
crystal size, mm^3	0.52 × 0.34 × 0.20	0.46 × 0.40 × 0.30	0.24 × 0.12 × 0.08	0.48 × 0.40 × 0.20	0.30 × 0.24 × 0.20	0.40 × 0.28 × 0.20
final R indices [$I > 5\sigma(I)$]						
R1	0.0344	0.0299	0.0419	0.0347	0.0299	0.0401
wR2	0.0890	0.0770	0.0921	0.0865	0.0738	0.0983

Scheme 1. Preparation of 1,1,4,4-Tetra(1-pyrazolyl)butane, **L2** (Top), and 1,1,5,5-Tetra(1-pyrazolyl)pentane, **L3** (Bottom)

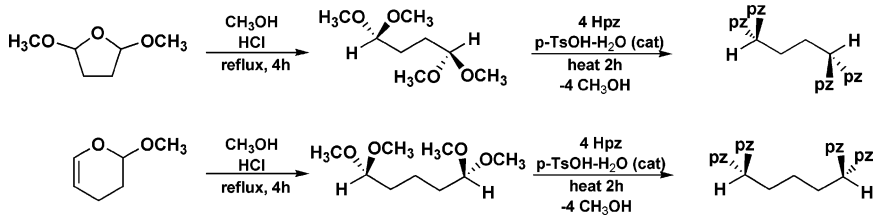

squares refinement of 6606, 9344, 9146, 5452, 8687, and 5556 reflections from the data sets of **1**−**6**, respectively, each with $I > 5(\sigma)I$. Analysis of the data showed negligible crystal decay during collection. Empirical absorption corrections were applied with SADABS[17] in the cases of **1**, **4**, and **6**, but none was applied to **2**, **3**, or **5**. Direct methods structure solution, difference Fourier calculations, and full-matrix least-squares refinement against F^2 were performed with SHELXTL.[17] All non-hydrogen atoms were refined with anisotropic displacement parameters except where noted. Hydrogen atoms were placed in geometrically idealized positions and included as riding atoms. Details of the data collection are given in Table 1 while further notes regarding the structure solution and refinement for **1**−**6** follow.

Compound **1** crystallizes in the triclinic system. The space group $P\bar{1}$ was assumed and confirmed by the successful solution and refinement of the data. The asymmetric unit consists of the $[Ag_2(\mu\text{-}\mathbf{L2})_2]^{2+}$ cation, two independent BF_4^- counterions, and half of a CH_3CN molecule of crystallization. One of the BF_4^- groups (B2) is disordered. A disorder model incorporating three distinct orientations was used, with the aid of 60 restraints to maintain reasonable geometry for all components. Occupancies were initially refined but eventually fixed near the refined values (A/B/C = 0.40/0.25/0.35). The CH_3CN molecule is disordered about an inversion center.

For compound **2**, systematic absences in the intensity data indicated either of the space groups *Cc* or *C*2/*c*, the latter of which was eventually confirmed. One complete $[Ag_2(\mu\text{-}\mathbf{L2})_2]$ complex, two triflate anions, and a half of a disordered CH_2Cl_2 molecule were located in the asymmetric unit. The CH_2Cl_2 molecule is disordered about a 2-fold axis. The C−Cl distances for this species were restrained to be similar (SHELX SADI). Another region of electron density is present, presumably solvent, which could not be identified due to severe disorder. The program SQUEEZE was used to account for these species. Squeeze calculated a solvent-accessible region of 753.4 Å^3 (7.8% of the total cell volume) corresponding to 271 e$^-$ per unit cell. Note that the tabulated crystallographic data reflect only the known cell contents.

Compound **3** crystallizes in the space group $P2_1/c$ as determined by the pattern of systematic absences in the intensity data. The asymmetric unit consists of one Ag center, one complete **L2** ligand, half of another **L2** ligand located on an inversion center, and one NO_3^- counterion.

Compound **4** crystallizes in the triclinic system. The space group $P\bar{1}$ was assumed and confirmed by the successful solution and refinement of the data. The asymmetric unit consists of the $[Ag_2(\mu\text{-}\mathbf{L3})_2]^{2+}$ cation and two BF_4^- anions. All species reside on positions of general crystallographic symmetry. One of the BF_4^- anions (B2) is disordered over two orientations in the refined ratio 0.764(6)/0.236(6) (A/B). The geometries of both components of this group were restrained to be similar to that of the regular anion B1 (30 restraints). The minor disorder component of the disordered BF_4^- anion was refined with isotropic displacement parameters.

Compound **5** crystallizes in the space group $P2_1/n$ as determined uniquely by the pattern of systematic absences in the intensity data. The asymmetric unit consists of half a $[Ag_2(\mu\text{-}\mathbf{L3})_2]^{2+}$ cation located on an inversion center, a triflate counterion, and a CH_2Cl_2 molecule of crystallization.

Compound **6** crystallizes in the space group $P2_1/c$. The asymmetric unit consists of the monomeric unit $[Ag(\mu\text{-}\mathbf{L3})]^+$ and one NO_3^- counterion.

Results

Syntheses. The ligands **L2** and **L3** were prepared as shown in Scheme 1. A ring-opening methanolysis in the presence of HCl was used to convert 2,5,-dimethoxytetrahydrofuran

(17) Sheldrick, G. M. *SHELXTL* version 6.1; Bruker Analytical X-ray Systems, Inc.: Madison, WI, 2000.

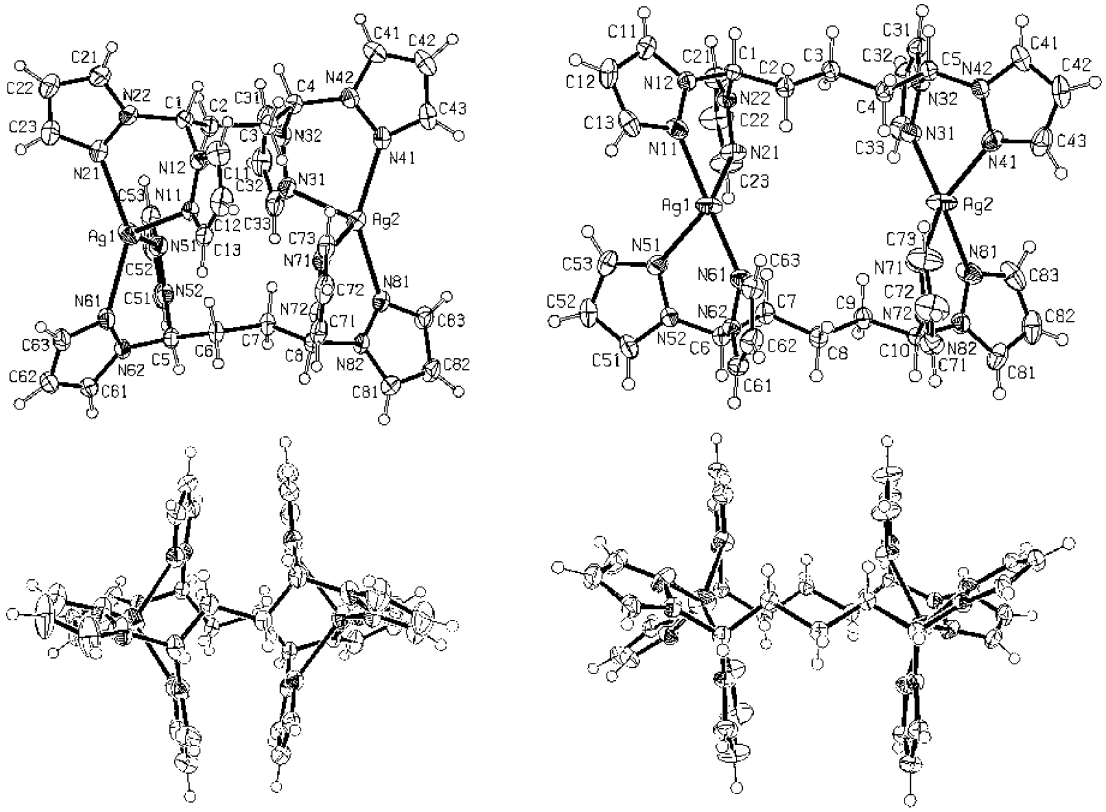

Figure 3. Orthogonal views of the cations in $\{Ag_2[\mu\text{-}CH(pz)_2(CH_2)_2CH(pz)_2]_2\}(BF_4)_2 \cdot 0.5CH_3CN$ (**1**) and $\{Ag_2[\mu\text{-}CH(pz)_2(CH_2)_3CH(pz)_2]_2\}(BF_4)_2$ (**4**).

to succinaldehyde bis(dimethylacetal), and the ligand **L2** was produced by the methanol elimination reaction between the acetal and pyrazole with catalytic *p*-toluenesulfonic acid (*p*-TsOH). Similarly, 2-methoxy-3,4-dihydro-2*H*-pyran was converted to glutaraldehyde bis(dimethylacetal) by a reported procedure,[15] and this acetal was subsequently converted to **L3**. The methanol elimination reactions were both complete within 2 h, markedly faster than the reaction to make **L1**. Both ligands are readily soluble in most polar organic solvents, although somewhat less soluble in CH_2Cl_2 and Et_2O than acetone or acetonitrile. In all solvents, **L3** is notably more soluble than **L2**.

The silver complexes of both ligands were prepared by dissolving both ligand and silver salt together in a minimum amount of acetonitrile (for $AgBF_4$ and $AgNO_3$) or CH_2Cl_2 (for $AgSO_3CF_3$) and allowing Et_2O to slowly diffuse into these solutions. Crystals formed within 1−2 days. The $AgNO_3$ complex of **L2** is the least soluble of all the compounds, being insoluble in all common organic solvents except acetonitrile and DMSO, in which solvents it is slightly soluble. The other silver complexes of **L2** are soluble in acetonitrile with gentle heating. The silver complexes of **L3** are soluble in acetonitrile without heating, except for the $AgNO_3$ complex, which does require heating to dissolve. X-ray structural and mass spectral measurements (vide infra) indicated the following compositions: $[Ag_2(\mathbf{L2})_2](BF_4)_2 \cdot 0.5CH_3CN$ (**1**), $[Ag_2(\mathbf{L2})_2](SO_3CF_3)_2 \cdot 0.5CH_2Cl_2$ (**2**), $[Ag_2(\mathbf{L2})_3](NO_3)_2$ (**3**), $[Ag_2(\mathbf{L3})_2](BF_4)_2$ (**4**), $[Ag_2(\mathbf{L3})_2](SO_3CF_3)_2 \cdot 2CH_2Cl_2$ (**5**), $[Ag(\mathbf{L3})]NO_3$ (**6**). Elemental analyses on dried crystalline samples confirmed these formulas except for compounds **2** and **5**, whose elemental analyses indicated that the solvent of crystallization was lost upon drying under high vacuum (1 mmHg). In compound **2**, the unidentified solvent region observed in the crystal structure was also lost upon drying.

NMR. Because of the limited solubility of the silver nitrate complex of **L2**, its ^{13}C NMR spectrum could not be obtained. The ^1H and ^{13}C NMR spectra of the remaining complexes showed only one set of resonances at room temperature, where most or all the signals were shifted downfield from those of the free ligand. These results are in agreement with the established lability of silver pyrazolyl complexes and with our previous observations. The ^{19}F NMR spectra of the $AgSO_3CF_3$ complexes also show only one signal as expected, but those of the $AgBF_4$ complexes show two signals in a 20:80 ratio due to the isotope effect from the adjacent boron whose isotopes, ^{10}B and ^{11}B, have a 20:80 ratio of natural abundances.

Solid-State Structures. Noncoordinating Anions (BF_4^-, $SO_3CF_3^-$). The $AgBF_4$ and $AgSO_3CF_3$ complexes of **L2** and **L3** crystallize with discrete macrocylic cations in which two ligand molecules, bidentate at both ligating sites, are bridging two silvers whose coordination geometries are distorted tetrahedral. Figure 3 (left) shows the cation from the crystal structure of **1**. The structure of **2** as a solvate of unknown composition (either Et_2O, CH_2Cl_2 or a mixture of both) contains analogous cations. The cyclic unit of **4** is shown in Figure 3 (right). The structure of **5** contains similar cations.

Table 2. Selected Bond Distances and Angles for **1**, **2**, **4**, and **5**

	1	2	4	5
Ag(1)−N(11)	2.343(2)	2.247(2)	2.305(2)	2.5092(19)
Ag(1)−N(21)	2.285(2)	2.4039(18)	2.351(2)	2.2385(18)
Ag(1)−N(51)	2.331(2)	2.237(2)	2.378(2)	
Ag(1)−N(61)	2.286(2)	2.3998(19)	2.248(2)	
Ag(1)−N(41*)				2.3151(17)
Ag(1)−N(31*)				2.3413(18)
Ag(2)−N(31)	2.380(2)	2.2603(17)	2.234(2)	
Ag(2)−N(41)	2.236(2)	2.4239(19)	2.377(3)	
Ag(2)−N(71)	2.368(2)	2.301(2)	2.283(2)	
Ag(2)−N(81)	2.261(2)	2.3269(19)	2.317(3)	
N(11)−Ag(1)−N(21)	85.31(8)	85.55(6)	85.62(8)	83.10(6)
N(11)−Ag(1)−N(31*)				90.70(6)
N(41*)−Ag(1)−N(11)				132.83(6)
N(11)−Ag(1)−N(51)	118.46(7)	148.69(8)	124.01(8)	
N(11)−Ag(1)−N(61)	115.04(7)	106.67(7)	129.99(8)	
N(21)−Ag(1)−N(31*)				143.83(7)
N(21)−Ag(1)−N(41*)				124.51(7)
N(21)−Ag(1)−N(51)	110.38(8)	117.43(7)	94.71(8)	
N(21)−Ag(1)−N(61)	143.94(8)	108.30(6)	136.02(8)	
N(31*)−Ag(1)−N(41*)				85.11(6)
N(51)−Ag(1)−N(61)	86.65(7)	86.94(7)	85.28(8)	
N(31)−Ag(2)−N(41)	86.32(8)	82.95(6)	86.61(8)	
N(31)−Ag(2)−N(71)	109.02(7)	140.79(6)	142.99(9)	
N(31)−Ag(2)−N(81)	112.89(7)	128.13(6)	115.79(9)	
N(41)−Ag(2)−N(71)	117.25(8)	104.13(7)	101.81(8)	
N(41)−Ag(2)−N(81)	144.39(8)	114.90(7)	129.63(9)	
N(71)−Ag(2)−N(81)	85.70(7)	84.41(7)	86.49(9)	

Selected bond lengths and angles are provided in Table 2. In each of the complexes **1**, **2**, **4**, and **5**, the coordination of the pyrazolyl nitrogen atoms about silver is slightly asymmetric in the two Ag−N bonds associated with each bis(pyrazolyl)methane unit: one is longer than the other. For example, in **1** the Ag(1)−N(11) distance is 2.343(2) Å whereas the Ag(1)−N(21) distance is 2.285(2) Å. Also, in the same compound, the Ag(2)−N(31) distance is 2.380(2) Å whereas the Ag(2)−N(41) distance is 2.236(2) Å. Each silver atom in the complexes acts as a spiro-atom fusing two chelate rings in boat conformations. The bite angles in these complexes range from 83° to 87° and are consistent with previously described complexes.[11,12]

One interesting observation is that the distance between the silver atoms in these macrocycles remains fairly constant (6.02 Å for **1**, 6.16 Å for **2**, 6.16 Å for **4**, and 6.42 for **5**) despite the addition of a methylene unit when substituting **L2** for **L3**. This may be contrasted with the large jump in metal−metal separation between the **L2** to **L1** derivatives where the latter were in the range 3.73−4.03 Å.

Supramolecular Structures. The supramolecular structure of **1** consists of layered sheets in the *ab*-plane that stack along the *c*-axis with no significant noncovalent interactions between the layers (Figure 4). The cyclic cations are linked into chains along the *a*-axis by a modified pyrazolyl embrace that displays edge to face CH···π interactions where two hydrogen atoms (rather than one) are interacting with the π clouds of the hydrogen-accepting pyrazolyl rings. Thus, both H(51) and H(52) are interacting with the π cloud of the pyrazolyl ring containing N(81) and N(82) with an edge to face distance of 3.63 Å, and H(71) and H(72) are interacting with the pyrazolyl ring containing N(61) and N(62) with an edge to face distance of 3.47 Å. The π···π stacking

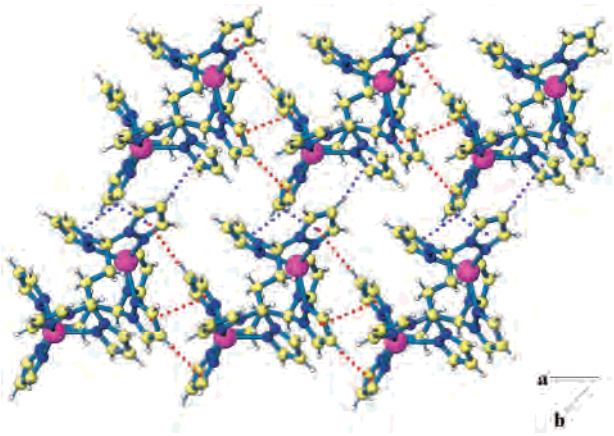

Figure 4. View of the *ab*-plane of **1** showing sheets formed from the pyrazolyl embrace (red dashed lines) and CH···π interactions (blue dashed lines).

component is within the expected ranges for these interactions (centroid···centroid distance of 3.72 Å, ⊥ interplane distance of 3.64 Å, dihedral angle $\alpha = 14.6°$, slip angle $\beta = 11.1°$). In addition to the pyrazolyl embrace, two CH···π interactions connect each macrocycle to an adjacent one along the *b*-axis. One interaction is between H(22), which is at the pyrazolyl 4-C position, and the π cloud of the pyrazolyl ring containing N(31) on an adjacent dimer (CH···centroid distance of 2.82 Å). The other is a bifurcated CH···π interaction between H(83), at the pyrazolyl 3-C position, and the two pyrazolyl rings containing N(11) and N(21) (CH···centroid distances of 2.86 and 2.98 Å). Thus, the pyrazolyl embrace along *a* and the CH···π interactions along *b* organize the dimeric cations into two-dimensional sheets. There is no significant interaction between the BF_4^- anions and the dimeric cations, although the counterions do exhibit short CH···F distances of <2.5 Å[18] with the acetonitrile molecules present in the structure. One of the two distinct kinds of BF_4^- molecules present in the crystal is disordered.

Complex **2** crystallizes from CH_2Cl_2/Et_2O in the space group *C*2/*c* with half a molecule of CH_2Cl_2 per asymmetric unit as well as an unidentified disordered solvate (either CH_2Cl_2 or Et_2O). The three-dimensional extended structure of **2** is unlike that of **1** in that there are no pyrazolyl embrace interactions. Rather, it comprises multiple noncovalent interactions that include significant weak hydrogen bonds with the $SO_3CF_3^-$ counterions (Table 3). These latter interactions occur between oxygen atoms of the $SO_3CF_3^-$ anions and both the methine and pyrazolyl 5-C hydrogens to create chains of cycles running in the *ac*-plane (Figure 5). In addition, CH···π interactions, involving only the pyrazolyl 4-C hydrogen atoms as the donor, extend in all dimensions of the structure and include a 3.05-Å interaction between H(22) and the pyrazolyl ring containing N(31) and a 3.38-Å interaction between H(12) and the pyrazolyl ring containing N(81). A pyrazolyl 5-C hydrogen, H(13), also forms a 3.32-Å CH···π interaction with the pyrazolyl ring containing N(71).

(18) Grepioni, F.; Cojazzi, G.; Draper, S. M.; Scully, N.; Braga, D. *Organometallics* **1998**, *17*, 296.

Table 3. Details of Hydrogen Bonding Interactions for **2**−**5**

D−H···A	H···A/Å	D···A/Å	D−H···A/deg
	Compound **2**		
C(1)−H(1)···O(1)	2.38	3.35	165
C(4)−H(4)···O(2)	2.26	3.24	166
C(5)−H(5)···O(5)	2.37	3.15	134
C(8)−H(8)···O(4)	2.33	3.33	174
C(31)−H(31)···O(1)	2.42	3.36	167
C(61)−H(61)···O(6)	2.36	3.16	141
	Compound **3**		
C(1)−H(1)···O(2)	2.44	3.38	162
C(2)−H(2)···O(3)	2.35	3.28	155
C(11)−H(11)···O(3)	2.50	3.28	141
C(12)−H(12)···O(2)	2.48	3.35	155
C(23)−H(23)···O(1)	2.28	3.11	147
C(41)−H(41)···O(3)	2.40	3.18	140
	Compound **4**		
C(5)−H(5)···F(2)	2.44	3.30	144
C(22)−H(22)···F(2)	2.47	3.34	153
C(71)−H(71)···F(4)	2.30	3.10	143
	Compound **5**		
C(1)−H(1)···O(1)	2.32	3.28	163
C(5)−H(5)···O(3)	2.49	3.42	153
C(41)−H(41)···O(3)	2.41	3.22	143
C(31)−H(31)···O(2)	2.40	3.35	171
C(43)−H(43)···F(1)	2.43	3.18	136

Complex **4** crystallizes in the space group $P\bar{1}$, and one of the two BF_4^- anions in the asymmetric unit is disordered. Noncovalent interactions involving the pyrazolyl rings of the cations and also the BF_4^- anions impart a 3-D extended structure onto crystals of complex **4**. Table 3 provides a summary of these interactions. The pyrazolyl embrace holds together one-dimensional chains of the cyclic dimers along the *a*-axis. The embrace is between the pyrazolyl 4-C hydrogen, H(42), and the ring containing N(61) (distance 2.91 Å, $\theta = 137.8°$) and between the pyrazolyl 4-C hydrogen, H(52), and the ring containing N(31) (distance 2.74 Å, $\theta = 142.4°$). The centroids of the rings containing N(41) and N(51) stack at a distance of 3.56 Å, with $\beta = 11.3°$ and $\perp$ interplane distance of 3.49 Å. Two CH···π interactions involving both pyrazolyl 4-C hydrogens (3.04 Å) and pyrazolyl 3-C hydrogens (3.02 Å) create sheets of dimers in the *ab*-plane. Finally, the structure is extended into

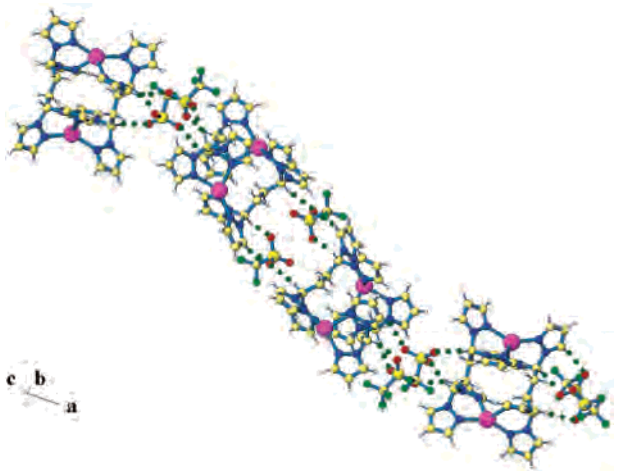

Figure 5. Chain in the *ac*-plane of $\{Ag_2[\mu\text{-}CH(pz)_2(CH_2)_2CH(pz)_2]_2\}(SO_3CF_3)_2 \cdot 0.5CH_2Cl_2$ (**2**) created by CH···O interactions (green dashed lines) between the cationic macrocycles and the $SO_3CF_3^-$ anions.

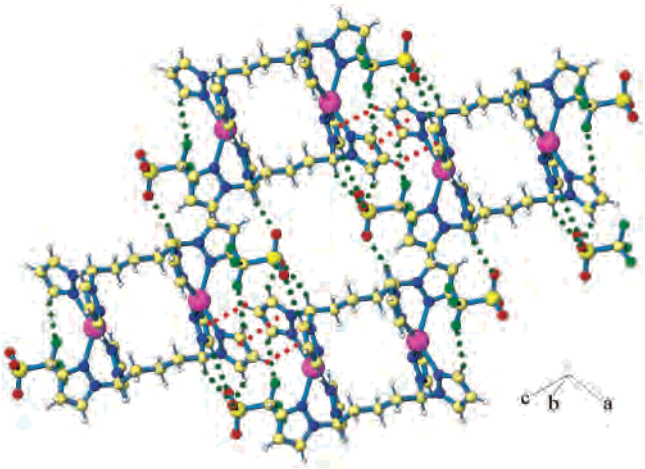

Figure 6. Sheets in the *ac*-plane of $\{Ag_2[\mu\text{-}CH(pz)_2(CH)_3CH(pz)_2]_2\}(SO_3CF_3)_2 \cdot 2CH_2Cl_2$ (**5**) formed by interactions between the cationic macrocycle and triflate anions (green dashed lines). The pyrazolyl embrace is shown by the red dashed lines.

the third dimension by CH···F interactions[18] between the BF_4^- anions and the pyrazolyl 3-C, 4-C, and methine, C*H*$(pz)_2$, hydrogens that create sheets in the *bc*-plane of the crystal.

Complex **5** crystallizes in the space group $P2_1/n$ where the center of each macrocycle resides on an inversion center. Complex **5**, in contrast to **4** but similar to **1**, lacks extended 3-D structure but instead consists of layers of sheets in the *ac*-plane that pack along the *c*-direction without close noncovalent interactions (Figure 6). As in structure **4**, chains of the cationic dimers are held together along the *a*-axis by the pyrazolyl embrace (H(42)-centroid with N(31) distance 2.84 Å, $\theta = 139.0°$; $\pi\cdots\pi$ stacking distance 3.52 Å, $\beta = 13.2°$, $\perp$ interplane distance of 3.43 Å). Oriented along the *c*-axis are weak CH···O hydrogen bonding interactions (Table 3) between the $SO_3CF_3^-$ oxygens and the pyrazolyl 3-C, pyrazolyl 5-C, and methine hydrogen atoms. The so-formed sheets in the *ac*-plane are further supported by several short CH···F interactions (<2.5 Å).[18]

Silver Nitrate Complexes. The structure of the $AgNO_3$ complex of **L2** has the empirical formula $\{Ag_2[\mu\text{-}CH(pz)_2(CH_2)_2CH(pz)_2]_3\}(NO_3)_2$ (**3**) with three ligand molecules per two silver atoms. The asymmetric unit is shown in Figure 7 (top) while selected distances and angles are given in Table 4. The asymmetric unit consists of one (type A) of the two ligands that comprise a macrocycle, and one-half of the ligand (type B) that resides on an inversion center and that links the macrocycles. The macrocyclic dication is related to those described for **1** and **2**, but in the current structure the macrocycle is composed of ligands that are bidentate on one end and monodentate on the other. These cycles are covalently linked to form a coordination polymer running along the *b*-axis by a second distinct ligand molecule that binds in a monodentate fashion on each end as in Figure 7 (bottom).

The 3-D extended structure of **3** is supported by weak CH···π and CH···O hydrogen bonding interactions (Table 3), but there is neither a pyrazolyl embrace nor any other $\pi\cdots\pi$ stacking interactions. Along the *a*-axis are bifurcated

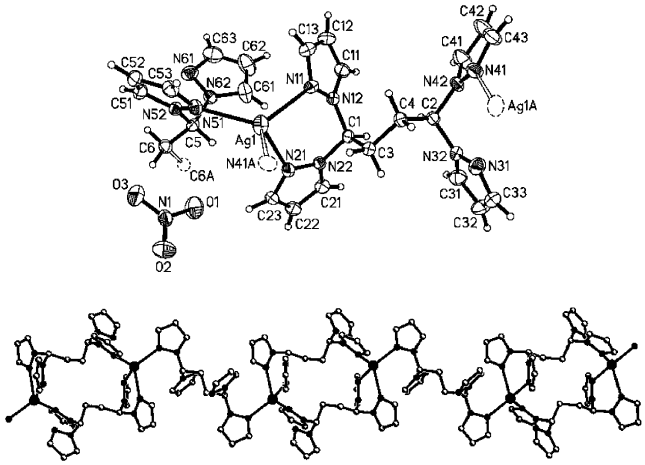

Figure 7. View of the asymmetric unit of $\{Ag_2[\mu\text{-}CH(pz)_2(CH_2)_2CH(pz)_2]_3\}(NO_3)_2$ (**3**) (top) and of the coordination polymer chain running along the *b*-axis (bottom).

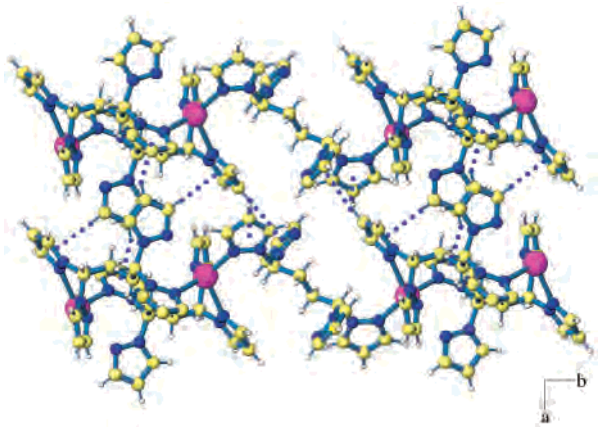

Figure 8. View of the *ab*-plane of **3** showing bifurcated and single CH···π interactions (blue dashed lines) between the polymeric chains.

Table 4. Selected Bond Distances and Angles for **3**

Ag(1)−N(11)	2.369(3)
Ag(1)−N(21)	2.515(3)
Ag(1)−N(31*)	2.930(3)
Ag(1)−N(41*)	2.326(3)
Ag(1)−N(51)	2.288(2)
N(11)−Ag(1)−N(21)	79.37(9)
N(11)−Ag(1)−N(31*)	82.33(9)
N(11)−Ag(1)−N(41*)	122.15(9)
N(11)−Ag(1)−N(51)	121.45(9)
N(21)−Ag(1)−N(31*)	154.96(8)
N(21)−Ag(1)−N(41*)	101.79(10)
N(51)−Ag(1)−N(21)	117.17(8)
N(31*)−Ag(1)−N(41*)	73.91(9)
N(31)−Ag(1)−N(51*)	87.02(8)
N(41)−Ag(1)−N(51*)	109.24(10)

CH···π interactions between H(22), which is at the pyrazolyl 4-C position of a type A ligand molecule, and the pyrazolyl rings containing N(51) and N(61) of a type B ligand molecule in an adjacent chain. There are also CH···π interactions between hydrogens at the 3-C (H(33)) and 4-C (H(32)) positions of a type A pyrazolyl ring not coordinated to Ag and the two nearest pyrazolyl rings in an adjacent dimer along *a*. Figure 8 shows the CH···π interactions in the *ab*-plane. In the *bc*-plane, CH···π interactions exist between a pyrazolyl 4-C hydrogen (H(62)) of an uncoordinated pyrazolyl ring in a type B ligand molecule with an uncoordinated pyrazolyl ring containing N(31) of a type A ligand molecule, thus completing the 3-D structure of the cationic polymers. The structure is supported in the *bc*-plane by O···H weak hydrogen bonds between the nitrate anions and both the methine hydrogen and pyrazolyl 4-C and 5-C hydrogen atoms, which propagate along the *c*-axis and *b*-axis, respectively. The pyrazolyl CH···O interactions involve both coordinated and uncoordinated pyrazolyl rings.

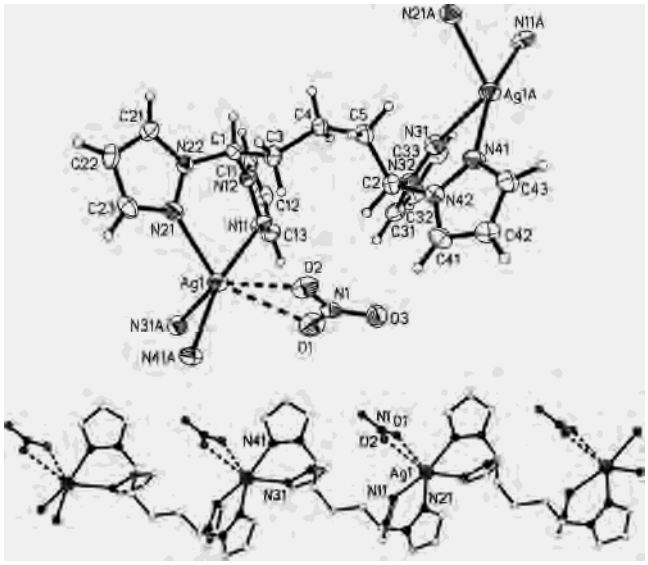

Figure 9. Top: ORTEP drawing of $\{Ag[CH(pz)_2(CH_2)_3CH(pz)_2]\}NO_3$ (**6**). Bottom: View of coordination polymer with silver-coordinated nitrate anions.

Table 5. Selected Bond Distances and Angles for **6**

Ag(1)−N(11)	2.419(3)
Ag(1)−N(21)	2.372(3)
Ag(1)−N(41*)	2.361(3)
Ag(1)−N(31*)	2.502(3)
Ag(1)−O(1)	2.887(3)
Ag(1)−O(2)	2.724(3)
N(1)−Ag(1)−N(21)	82.68(9)
N(11)−Ag(1)−N(31*)	100.86(10)
N(41*)−Ag(1)−N(11)	165.46(10)
N(21)−Ag(1)−N(31*)	113.76(10)
N(41*)−Ag(1)−N(21)	109.93(10)
N(31*)−Ag(1)−N(41*)	81.04(10)
N(11)−Ag(1)−O(1)	145.05(9)
N(11)−Ag(1)−O(2)	83.24(9)
N(21)−Ag(1)−O(1)	145.05(9)
N(21)−Ag(1)−O(2)	106.24(9)
N(31*)−Ag(1)−O(1)	96.89(8)
N(31*)−Ag(1)−O(2)	140.00(8)
N(41*)−Ag(1)−O(1)	90.38(9)
N(41*)−Ag(1)−O(2)	86.16(9)
O(1)−Ag(1)−O(2)	45.23(7)

The $AgNO_3$ complex of **L3** is markedly different from the previous five complexes in that it crystallizes in the space group $P2_1/c$ as a coordination polymer with the empirical formula $\{Ag[\mu\text{-}CH(pz)_2(CH_2)_3CH(pz)_2]\}NO_3$ where the repeat chain units propagate along the *a*-axis instead of forming macrocyclic cationic units. Views of the coordination polymer can be seen in Figure 9 while Table 5 provides selected bond distances and angles. Each bis(pyrazolyl)methane unit coordinates in a bidentate fashion, and a weakly

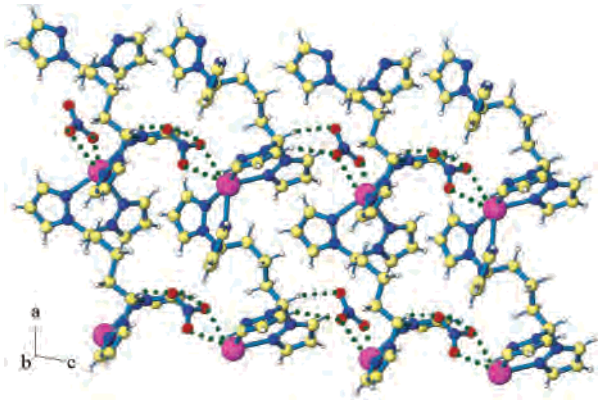

Figure 10. View of the *ac*-plane of **6** showing coordination of the nitrate anions to the silver cations as well as nitrate−ligand hydrogen bonding (green dashed lines).

bonded, bidentate nitrate contributes to a pseudo-octahedral environment around silver. As in the previous complexes, the coordination of the bis(pyrazolyl)methane units to each silver atom is asymmetric. The asymmetry is more pronounced in **6**, however. The Ag(1)−N(11) distance is 2.419(3) Å, but the Ag(1)−N(21) distance is 2.372(3) Å; also, the Ag(1)−N(31*) distance is 2.502(3) Å, but the Ag(1)−N(41*) distance is 2.361(3) Å. The Ag−O bonds arising from nitrate coordination are also of different lengths (Ag(1)−O(1) = 2.887(3) Å, Ag(1)−O(2) = 2.724(3) Å), though not quite so distinct as is found for anisobidentate nitrate coordination.[8a]

The supramolecular structure is three-dimensional. A combination of CH···O and Ag−O interactions with the nitrate ions (Figure 10) joins adjacent chains creating sheets in the *ac*-plane. In addition, CH···π and π···π interactions also connect the chains along the *c*-axis, and other CH···π interactions connect the chains in the *b*-direction. There is no indication of any pyrazolyl embrace interactions.

Mass Spectra. The positive ion electrospray [ESI(+)] mass spectral experiments for compounds **1**−**5** all show weak peaks corresponding to the macrocyclic dimers associated with one counterion, i.e., $[\{Ag_2(\mathbf{L2})_2\}(BF_4)]^+$ for **1**, $[\{Ag_2(\mathbf{L2})_2\}(SO_3CF_3)]^+$ for **2**, $[\{Ag_2(\mathbf{L2})_2\}(NO_3)]^+$ for **3**, etc. The base peak was found to be either $[Ag(\mathbf{L2})]^+$ or $[Ag(\mathbf{L3})]^+$ for each of these complexes, as appropriate. Compound **6**, which is a simple coordination polymer, shows singular behavior compared to the other five complexes in that there is no peak corresponding to $[Ag_2(\mathbf{L3})_2(NO_3)]^+$. Again, the base peak corresponds to the monomer $[Ag(\mathbf{L3})]^+$, and there exists a weak peak for $[Ag(\mathbf{L3})_2]^+$.

Discussion

One goal of this study was to determine if lengthening the alkylidene spacer between the bis(pyrazolyl)methane ligating sites of **L1** from one CH_2 group to two and three, thus making the ligand more flexible, would produce silver complexes based on discrete cyclic dimers or instead lead to the production of simple coordination polymers. The four new complexes containing the weakly coordinating anions BF_4^- and $SO_3CF_3^-$ retain the cyclic dimeric structure observed with $\{Ag_2[CH_2(CH(pz)_2)_2]_2\}(SO_3CF_3)_2$ and $\{Ag_2(CH_2[CH(pz^{4Et})_2]_2)_2\}_3[Ag(NO_3)_4]_2$. The cyclic dimer structure is also observed in $\{Ag_2[\mu\text{-}CH(pz)_2(CH_2)_2CH(pz)_2]_3\}(NO_3)_2$ (**3**), but bonding of an additional ligand creates a coordination polymer of the cyclic dimers. Of the nine complexes we have prepared in this series, only the nitrate derivatives **6** and $[Ag_3\{\mu\text{-}CH_2[CH(pz)_2]_2\}_2](NO_3)_3(CH_3CN)_2$ do not have the cyclic structure, and these are the two complexes in which the nitrate directly bonds to the silver. In a sense, the nitrate anion serves to template the formation of coordination polymers or acyclic derivatives of these flexible ligands. Thus, it is clear that, in the absence of significant metal−anion interaction, the supramolecular isomer that is favored is the macrocyclic dimer, in these cases containing rings of 16, 18, and 20 atoms for the three ligands, respectively.

The ESI mass spectral data support the existence of the macrocyclic dimer structure in solution. For the seven complexes with that structure, peaks corresponding to the dimer, $[\{Ag_2(\mathbf{L})_2\}(\text{counterion})]^+$, are observed. In contrast, for **6** only monometallic peaks are observed. An indication that ESI mass spectral data are actually representative of the solution phase species is that in the trimeric complex $[Ag_3\{\mu\text{-}CH_2[CH(pz)_2]_2\}_2](NO_3)_3(CH_3CN)_2$ the timetallic cation $[Ag_3\mathbf{L2}(NO_3)_2]^+$ is observed.

The variation of the counterion along the series BF_4^-, $SO_3CF_3^-$, NO_3^-, which in addition to being the order of the tendency toward coordination to metals is the order of the tendency of these anions to enter into weak CH···X (X = F, O) hydrogen bonds, has an important influence on the supramolecular structures. In the two complexes of the BF_4^- anion, **1** and **4**, the main organizing feature of the supramolecular structure is the pyrazolyl embrace, outlined in Figure 2. In **1**, the counterion does not support the supramolecular structure although it does in **4**. In the two complexes of the $SO_3CF_3^-$ anion, **2** and **5**, weak hydrogen bonding forces are important in both supramolecular structures. In **2**, these forces dominate whereas in **5** both hydrogen bonding and the pyrazolyl embrace support the 2-D structure. The pyrazolyl embrace interaction is not present in either of the nitrate structures reported here, both of which are coordination polymers, although it is evident in the trimeric structure of $[Ag_3\{\mu\text{-}CH_2[CH(pz)_2]_2\}_2](NO_3)_3(CH_3CN)_2$.

In summary, the syntheses and structures of six silver(I) complexes of the new flexible alkylidene-linked bis(pyrazolyl)methane ligands $CH(pz)_2(CH_2)_nCH(pz)_2$ (n = 2, 3), with BF_4^-, $SO_3CF_3^-$, and NO_3^- as the counterions, are reported. Clearly, these types of ligands support the formation of $(Ag_2\mathbf{L2})^{2+}$ macrocycles, especially in complexes of weakly coordinating anions. Importantly, these types of ligands contain functional groups capable of supporting CH···π, π···π, and CH···X (X = F, O) hydrogen bonding interactions that support supramolecular structures. The quadruple pyrazolyl embrace interaction is frequently observed in these structures and is more likely to be the dominant force for counterions that can only weakly enter into CH···X (X = F, O) hydrogen bonds.

Acknowledgment. We thank the National Science Foundation (CHE-0414239) for support. We also thank the Alfred

P. Sloan Foundation and the EPSCoR program of the state of South Carolina for support of R.P.W. The Bruker CCD single crystal diffractometer was purchased using funds provided by the NSF Instrumentation for Materials Research Program through Grant DMR:9975623.

Supporting Information Available: X-ray crystallographic files in CIF format for all structures reported. This material is available free of charge via the Internet at http://pubs.acs.org.

IC0491377